Science Advances

AAAS

advances.sciencemag.org/cgi/content/full/3/10/e1701398/DC1

Supplementary Materials for

Three-dimensional supercritical resolved light-induced magnetic holography

Chenglong Hao, Zhongquan Nie, Huapeng Ye, Hao Li, Yang Luo, Rui Feng, Xia Yu, Feng Wen, Ying Zhang, Changyuan Yu, Jinghua Teng, Boris Luk'yanchuk, Cheng-Wei Qiu

Published 13 October 2017, *Sci. Adv.* **3**, e1701398 (2017)
DOI: 10.1126/sciadv.1701398

This PDF file includes:

Supplementary Text

Theoretical model for 4π microscopy and beams combination method

Before exploration of light-induced magnetization in the 4π beams combination configuration, it is prerequisite to investigate the relevant electric field distributions of a single high-NA objective. In principle, the effect of polarization should be taken into account in the high-NA geometry. When a linearly *x*-polarized plane wave illuminates an aplanatic lens, the electric fields **E** in the vicinity of the focus can be expressed according to Richards and Wolf (*42*) as

$$\mathbf{E}(r,\varphi,z)=\begin{bmatrix}e_x\\e_y\\e_z\end{bmatrix}=\begin{bmatrix}-iA(I_0+I_2\cos 2\varphi)\\-iAI_2\sin 2\varphi\\-2AI_1\cos\varphi\end{bmatrix} \tag{S1}$$

with

$$I_0=\int_0^{\alpha}P(\theta)(1+\cos\theta)\sin\theta J_0(kr\sin\theta)e^{ikz\cos\theta}\mathrm{d}\theta \tag{S2a}$$

$$I_1=\int_0^{\alpha}P(\theta)\sin^2\theta J_1(kr\sin\theta)e^{ikz\cos\theta}\mathrm{d}\theta \tag{S2b}$$

$$I_2=\int_0^{\alpha}P(\theta)(1-\cos\theta)\sin\theta J_2(kr\sin\theta)e^{ikz\cos\theta}\mathrm{d}\theta \tag{S2c}$$

where *A* is the field amplitude distribution at the pupil plane, α denotes the convergence semi-angle of the objective, $P(\theta)$ is the pupil apodization function, which is equal to $\cos^{1/2}\theta$ for the objective obeying the Abbe condition, J_n is the n$^{\text{th}}$-order Bessel function of the first kind, $k=2\pi/\lambda$ is the wave vector in image space. (r,φ,z) are cylindrical coordinates centered at the focus. Similarly, for a linearly *y*-polarized plane wave illumination, the electric fields $\mathbf{E}'$ in the vicinity of the focus can be expressed as

$$\mathbf{E}'(r,\varphi,z)=\begin{bmatrix}e'_x\\e'_y\\e'_z\end{bmatrix}=\begin{bmatrix}-iAI_2\sin 2\varphi\\-iA(I_0-I_2\cos 2\varphi)\\-2AI_1\sin\varphi\end{bmatrix} \tag{S3}$$

For a circularly polarized light, the Jones vector is expressed as

$$\mathbf{J}=\begin{bmatrix}\pm i\\1\end{bmatrix} \tag{S4}$$

where the + and – signs are corresponding to the left- and right-handed circular polarization, respectively. The circularly polarized light can be considered as the superposition of two orthogonally linearly polarized beams with π/2 phase retardation between them. Therefore, the electric field in the focus under left-handed circularly polarized incidence is obtained as

$$\mathbf{E}_{\mathrm{circ}}^{\mathrm{L}}\left(r,\varphi,z\right)=\begin{bmatrix}ie_x+e'_x\\ie_y+e'_y\\ie_z+e'_z\end{bmatrix}=\begin{bmatrix}A\left(I_0+I_2e^{-i2\varphi}\right)\\-iA\left(I_0-I_2e^{-i2\varphi}\right)\\-2AI_1e^{-i\varphi}\end{bmatrix} \tag{S5}$$

For the right-handed circularly polarized incidence we have

$$\mathbf{E}_{\mathrm{circ}}^{\mathrm{R}}\left(r,\varphi,z\right)=\begin{bmatrix}-ie_x+e'_x\\-ie_y+e'_y\\-ie_z+e'_z\end{bmatrix}=\begin{bmatrix}-A\left(I_0+I_2e^{i2\varphi}\right)\\-iA\left(I_0-I_2e^{i2\varphi}\right)\\2iAI_1e^{i\varphi}\end{bmatrix} \tag{S6}$$

To transform these electric-field components along the Cartesian-coordinate axes into their cylindrical-coordinate counterparts, we need to employ the following equation

$$\begin{bmatrix}E_r\\E_\varphi\end{bmatrix}=\begin{bmatrix}\cos\varphi & \sin\varphi\\-\sin\varphi & \cos\varphi\end{bmatrix}\begin{bmatrix}E_x\\E_y\end{bmatrix} \tag{S7}$$

The electric fields in the vicinity of the focus of left-handed and right-handed circularly polarized light in cylindrical coordinate are

$$\mathbf{E}_{\mathrm{circ}}^{\mathrm{L}}\left(r,\varphi,z\right)=\begin{bmatrix}E_r\left(r,\varphi,z\right)\\E_\varphi\left(r,\varphi,z\right)\\E_z\left(r,\varphi,z\right)\end{bmatrix}=Ae^{-i\varphi}\begin{bmatrix}\left(I_0+I_2\right)\\-i\left(I_0-I_2\right)\\-2iI_1\end{bmatrix} \tag{S8a}$$

and

$$\mathbf{E}_{\mathrm{circ}}^{\mathrm{R}}\left(r,\varphi,z\right)=\begin{bmatrix}E_r\left(r,\varphi,z\right)\\E_\varphi\left(r,\varphi,z\right)\\E_z\left(r,\varphi,z\right)\end{bmatrix}=Ae^{i\varphi}\begin{bmatrix}-\left(I_0+I_2\right)\\-i\left(I_0-I_2\right)\\2iI_1\end{bmatrix} \tag{S8b}$$

Essentially, the key to garner purely longitudinal magnetization all-optically in the magnetic hologram is to remove electric field along axial direction ($\boldsymbol{E}_z$). The 4π microscopic system is preferred due to its fascinating capability in achieving axial super-resolution simultaneously (*26*, *39*–*41*). In the 4π microscopic system, the electric fields near the foci are the superposition of the fields from two counter-propagating focused beams, which is (*47*)

$$\mathbf{E}_f\left(r,\varphi,z\right)=\mathbf{E}\left(r,\varphi,z\right)+\mathbf{E}\left(r,\varphi,-z\right) \tag{S9}$$

To achieve both perfect destructive interference of the axial electric field and constructive interference of the transverse counterpart at the focal plane, so as to make the pure transversally polarized optical field with sub-diffraction spot size possible, as well as inducing pure longitudinal magnetization via the inverse Faraday effect simultaneously, we propose 4π beams combination microscopic system. Therefore, the electric fields near foci are superposition of the multi-beams fields, shown in Fig. 1(a) in main text. That is

$$\mathbf{E}_t\left(r,\varphi,z\right)=\sum_{i=1}^{6}C_i\left[\mathbf{E}_i\left(r,\varphi,z\right)+\mathbf{E}_i\left(r,\varphi,-z\right)\right] \tag{S10}$$

where $\mathbf{E}_i$ stands for the focal electric fields with semi-aperture α_i. C_i denotes the amplitude modulation coefficient for corresponding beam. $-z$ in $\mathbf{E}_i$ indicates that the field is counter-propagating. In this article, the optimal semi-apertures and corresponding amplitude modulation coefficients are obtained through optimization.

Substituting Equation S8a into Equation S10, we obtain the electric field in the focal vicinity of this 4π beams combination microscopic system with left-handed circularly polarized plane wave illumination as

$$\mathbf{E}_{\mathrm{t}}^{\mathrm{LC}}\left(r,\varphi,z\right)=\begin{bmatrix}E_r\left(r,\varphi,z\right)\\E_\varphi\left(r,\varphi,z\right)\\E_z\left(r,\varphi,z\right)\end{bmatrix}=Ae^{-i\varphi}\begin{bmatrix}\left(H_0+H_2\right)\\-i\left(H_0-H_2\right)\\-2iH_1\end{bmatrix} \tag{S11}$$

Similarly, substituting Equation S8b into Equation S10, we obtain the electric field in the focal vicinity of this 4π beams combination microscopic system with right-handed circularly polarized plane wave illumination as

$$\mathbf{E}_{\mathrm{t}}^{\mathrm{RC}}\left(r,\varphi,z\right)=\begin{bmatrix}E_r\left(r,\varphi,z\right)\\E_\varphi\left(r,\varphi,z\right)\\E_z\left(r,\varphi,z\right)\end{bmatrix}=Ae^{i\varphi}\begin{bmatrix}-\left(H_0+H_2\right)\\-i\left(H_0-H_2\right)\\2iH_1\end{bmatrix} \tag{S12}$$

with H_{i} (i=0, 1, and 2) are three integrals of

$$H_0=\sum C_i\int_0^{\alpha_i}2\cos^{\frac{1}{2}}\theta\cos\left(kz\cos\theta\right)\sin\theta\left(1+\cos\theta\right)J_0\left(kr\sin\theta\right)\mathrm{d}\theta \tag{S13a}$$

$$H_1=\sum C_i\int_0^{\alpha_i}2\cos^{\frac{1}{2}}\theta\cos\left(kz\cos\theta\right)\sin^2\theta J_1\left(kr\sin\theta\right)\mathrm{d}\theta \tag{S13b}$$

$$H_2=\sum C_i\int_0^{\alpha_i}2\cos^{\frac{1}{2}}\theta\cos\left(kz\cos\theta\right)\sin\theta\left(1-\cos\theta\right)J_2\left(kr\sin\theta\right)\mathrm{d}\theta \tag{S13c}$$

Supercritical region criterion

For a spherical-lens-based optical imaging system, the light is usually focused into an Airy spot with the size of $0.61\lambda/NA$, accompanied by a very weak side lobe with a mere 1.75% intensity of main spot (*44*). Sub-diffraction limit focusing is feasible at the cost of increasing energy in the side lobes. For non-polarized incident light, higher spatial frequency corresponds to a smaller spot. The extreme case is that light with only the maximum spatial frequency is focused into a hotspot with intensity profile proportional to $\left|J_0\left(krNA\right)\right|^2$, which is named as "maximum-frequency spot". This maximum-frequency spot has a main lobe of $0.38\lambda/NA$ and comes with moderate side lobes (16.2% of main spot) (*45*, *46*). Following the same strategy, we examine the spot size that corresponds to single frequency with circularly polarized incident light. The minimum lateral spot size when the single frequency traverses from 0 to semi-aperture α, is taken as the super-oscillation criterion (SOC). The range of RC

to SOC can be defined as supercritical region. The mathematical description of SOC can be expressed as

$$\begin{aligned} &\text{Min} \quad \text{FWHM}\left(\text{I}(\theta)\right) \\ &\text{s.t.} \quad \theta \in [0, \alpha], \\ &\qquad \text{I}=I_0'^2 + 2I_1'^2 + I_2'^2 \end{aligned} \tag{S14}$$

with

$$I_0' = \cos^{\frac{1}{2}}\theta \sin\theta (1+\cos\theta) J_0(kr\sin\theta) \tag{S15a}$$

$$I_1' = \cos^{\frac{1}{2}}\theta \sin^2\theta J_1(kr\sin\theta) \tag{S15b}$$

$$I_2' = \cos^{\frac{1}{2}}\theta \sin\theta (1-\cos\theta) J_2(kr\sin\theta) \tag{S15c}$$

where α is the semi-aperture of objective. The $\text{FWHM}\left(\text{I}(\theta)\right)$ denotes the function which is employed to find the spot size at full width at half maximum. Figure S1 shows the resulted RC and SOC in our 4π system with oil-immersed objective (*NA*=1.43, $NA = 1.509 \times 0.95$). The SOC has a similar shape like the RC. For a given NA, the spot with size below the diffraction limit and above SOC can be called supercritical spot. What's more, the SOC for circularly polarized light is quite close to the SOC for non-polarized light when $\sin\alpha < 0.6$. The SOC is 0.3512λ and RC is 0.4255λ in our case ($NA = 1.509 \times 0.95$), thus, the resultant supercritical region is between 0.3512λ to 0.4255 λ. This finely distinguished roadmap provides an instructive guide that supercritical region is the best choice when one purses a super-resolution spot without high side lobes outside designed region. More importantly, this calculation method can be extended to incident light with other polarization modes, which provides a routine to find the SOC for different incident light.

Optimization on lateral supercritical design and axial side lobes suppression

The optimization target in our calculation is to minimize spot volume with following constrains. First, the minimum and maximum NA in beams combination is 0.981 ($\sin\alpha = 0.65$) and 1.434 ($\sin\alpha = 0.95$), respectively. Second, the lateral spot size is set to be in the supercritical region. Last, the side lobes should be below 30% of main spot, which is practical for real-life application. The optimization is implemented by using interior point

optimization algorithm, considering the beam sizes of six incident circularly polarized light and corresponding amplitude coefficients as optimizing parameters. The optimized parameters are shown in table S1.

Theory of light induced magnetization and magnetization reversal

Essentially, we treat conducting electrons within MO medium as a collisionless plasma in which the electrons can migrate freely (*25*, *43*). As a consequence, the effective magnetization, in the isotropic MO material, induced by incident beams in 4π beams combination system reads

$$\mathbf{M}\left(r,\varphi,z\right)=i\gamma\mathbf{E}_t\times\mathbf{E}_t^{*} \tag{S16}$$

where $\mathbf{E}_t^{*}$ denotes the complex conjugate of $\mathbf{E}_t$, γ is the magneto-optical susceptibility. Substituting Equations S11- S13 into Equation S16, and doing some simple mathematical simplifications, the induced magnetization fields by left-handed circularly polarized light and right-handed circularly polarized light in the 4π beams combination system are given by

$$\mathbf{M}_{\mathrm{LC}}\left(r,\varphi,z\right)=\begin{bmatrix}M_r\left(r,\varphi,z\right)\\M_\varphi\left(r,\varphi,z\right)\\M_z\left(r,\varphi,z\right)\end{bmatrix}=-2i\gamma A^2\begin{bmatrix}0\\2\left(H_0+H_2\right)H_1\\H_0^2-H_2^2\end{bmatrix} \tag{S17a}$$

and

$$\mathbf{M}_{\mathrm{RC}}\left(r,\varphi,z\right)=\begin{bmatrix}M_r\left(r,\varphi,z\right)\\M_\varphi\left(r,\varphi,z\right)\\M_z\left(r,\varphi,z\right)\end{bmatrix}=2i\gamma A^2\begin{bmatrix}0\\-2\left(H_0+H_2\right)H_1\\H_0^2-H_2^2\end{bmatrix} \tag{S17b}$$

with H_{i} (i=0, 1, and 2) in Equation S13.

Apparently, it is found from Equations S13 and S17 that the radial magnetization component disappears absolutely for both light helicity. Moreover, the induced total magnetization field is primarily determined by the longitudinal magnetization components as the value of H_0 always overwhelms that of either H_1 or H_2 in the focal region. Especially, the resultant magnetization field at r=0 and z=0 becomes totally longitudinal, i.e. $\mathbf{M}$=$\mathbf{M}_{\mathrm{z}}$, which is essentially different from the magnetization induced by single high-NA objective.

From Equation S17a and Equation S17b, one can immediately conclude that the magnetization direction under left-handed circularly polarized incident light is opposite to that under right-handed circularly polarized incident light at focal region at r=0 and z=0, i.e. $\mathbf{M}_{\mathrm{LC}} = -\mathbf{M}_{\mathrm{RC}}$. This theoretically proves that the magnetization reversal occurs via two illuminations with opposite light helicity (*18*).

Theoretical model for multifoci by multiple phase filters

To obtain desired multifoci pattern analytically, a common used routine is to convert the vectorial diffraction integral of Equations S1 and S2 into Fourier transform field $\mathbf{E_0}(x, y, z)$ (*48*, *49*). Thus, considering the incident beams modulated by multiple phase filters and following our previous analysis in (*50*), the focal distribution in Equation S1 can be rewritten as

$$\begin{aligned}\mathbf{E}(x, y, z) &= \iint \left[t(x, y)\mathbf{E_0}(x, y, z) \right] \exp\left[-i\left(k_x x + k_y y \right) \right] \mathrm{d}k_x \mathrm{d}k_y \\ &= FT\left\{ t(x, y) \right\} * FT\left\{ \mathbf{E_0}(x, y, z) \right\}\end{aligned} \tag{S18}$$

where *t(x, y)* is the transmittance function of MPFs, *FT*{} denotes the Fourier transform, the symbol * represents the convolution operation, and $\mathbf{E_0}(x, y, z)$ describes the weighted field with a vector angular spectrum form, which is

$$\mathbf{E_0}(x, y, z) = \left(\mathbf{e}_x + i\mathbf{e}_y \right) \exp\left(ik_z z \right) \Big/ \cos\theta \tag{S19}$$

where $\mathbf{e}_x$ and $\mathbf{e}_y$ are unit vectors in the x and y directions at the back aperture plane, respectively. $\mathrm{k} = \left(k_x, k_y, k_z \right)$ is the wave vector. As can be seen from Equation S18, the distribution of the focused field is represented as a spatial convolution with Fourier transform of *t(x, y)* and Fourier transform of $\mathbf{E_0}(x, y, z)$. This implies that it is feasible to focus light into multifocal spots provided that Fourier transform of *t(x, y)* exhibits a multifocal function. In a similar fashion, the super-resolved magnetization spot array can be generated by focusing circularly polarized light beams impinging on the proposed multiple phase filters. To this end, the following analytical formula is given as

$$t(x, y) = \sum_{i=1}^{N} \exp\left[-ik\left(a_i x + b_i y \right) \right] \times \exp\left(-ikc_i \cos\theta \right) \tag{S20}$$

where N is an integer, giving the total number of spots along the x, y and z directions; a_i, b_i and c_i represent the displacements along x, y and z directions, respectively. Combining Equations S16, S17 and Equations S18 to S20, the multifoci magnetization spots can be produced by focusing left-handed circularly polarized plane beam imposed by the multiple phase filters, which is shown in Fig. 3 and Fig. 2.

GPU parallel computing

When the multifocal off-axial magnetization spots are numerically generated, it includes time-consuming double integral in Debye vectorial diffraction theory. Calculation based on Fast Fourier Transform was proposed to accelerate the computing speed. However, the results from this method are accurate only under the given sampling conditions. Therefore, another route, which is more general and fast compared with normal calculation, is desired. Here, we propose to use GPU parallel computing to accelerate computing speed of the double integral. The double integral is programmed with GPU array and parallel computing on the platform of Matlab 2016a (www.mathworks.com/videos/parallel-computing-tutorial-gpu-computing-with-matlab-9-of-9-91572.html). The computing speed is accelerated by ~15 times compared with CPU computing. The performances of GPU parallel computing vs. CPU computing are listed in the table S2. From table S2, the conclusion can be drawn that GPU parallel computing greatly accelerate calculation speed to ~15 times, which can potentially be a new routine for massive calculation.

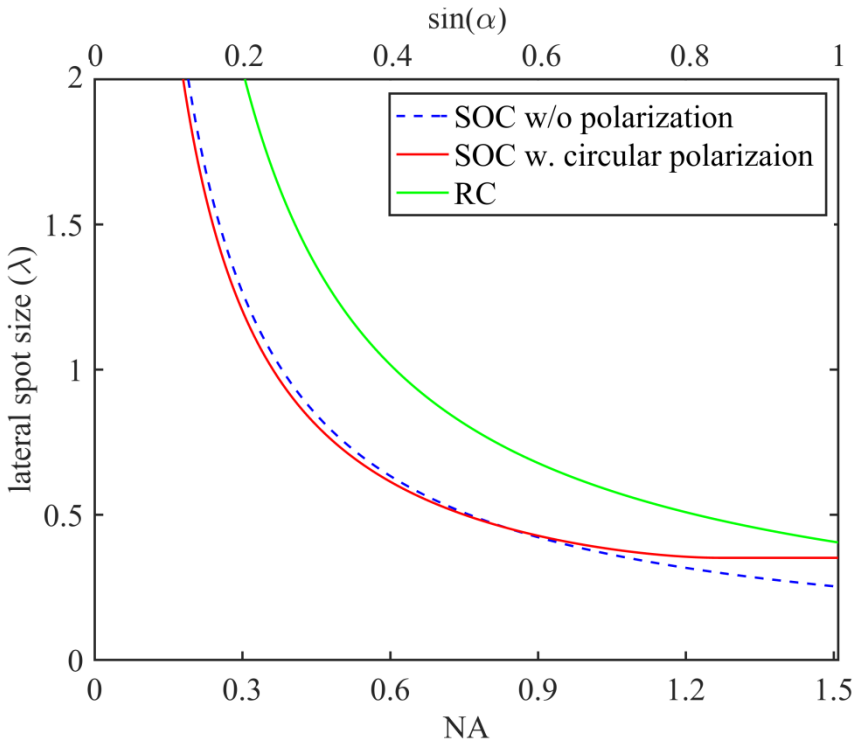

fig. S1. The lateral spot size as a function of NA under a circularly polarized light illumination. The red curve indicates the super-oscillation criterion (SOC). The green curve indicates the Rayleigh Criterion (RC). The region below SOC is super-oscillation, the region between red curve and green curve is supercritical region under circularly polarized light illumination. The blue dash line indicates the SOC for non-polarized light. The difference between SOC for circularly polarized light and SOC for non-polarized light is relative small when NA is less than 0.9 ($\sin\alpha < 0.6$).

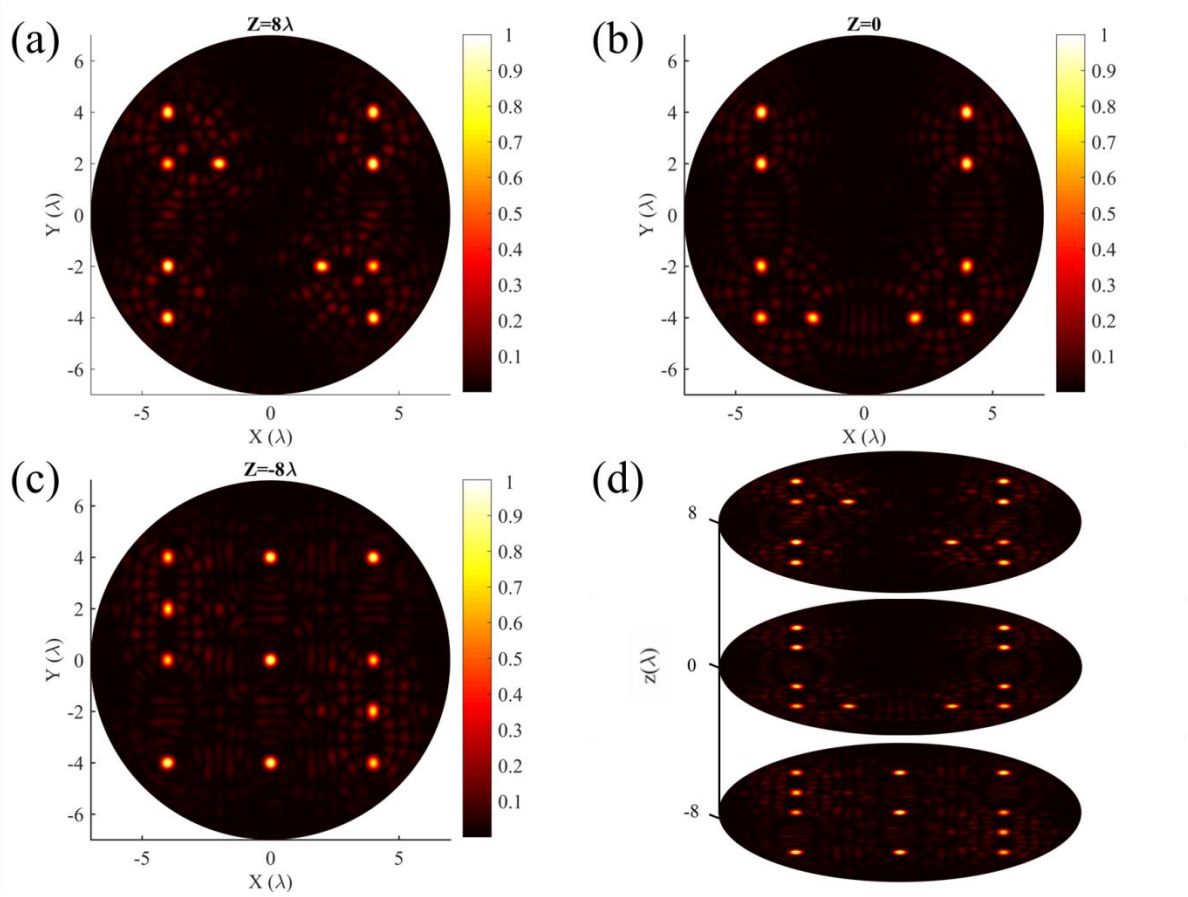

fig. S2. The logo of NUS in the focal region. (**a**) The capital letter "N" in XY plane at Z=8λ with 10 MSs; (**b**) The capital letter "U" in XY plane at Z=0 with 10 MSs; (**c**) The capital letter "S" in XY plane at Z=-8λ with 11 MSs; (**d**) The 3D slice of logo NUS in the focal region.

table S1. Optimized parameters (α_i and C_i) for supercritical MS generation.

	1	**2**	**3**	**4**	**5**	**6**
Aperture (α_i rad)	0.6546	0.6819	0.7002	0.7617	0.7795	0.9452
Amplitude modulation coefficients (C_i)	-0.4843	0.1292	-0.4000	0.7541	0.6152	-1.0000

table S2. Performance comparison: CPU computing versus GPU parallel computing.

	Pyramid (5 spots, calculating at Plane ABCD)	**NUS logo (31 spots calculation at "N" plane)**	**NUS logo (31 spots calculation at "U" plane)**	**NUS logo (31 spots calculation at "S" plane)**
Calculation time (hour): CPU: i7-6700 8M Cache, @3.4 GHz up to 4.00 GHz, with 16G RAM	25.75	152.46	142.38	160.2
Calculation time (hour):GPU: Geforce GTX 1070 1920 cores @1.5GHz, with 8GB RAM	1.79 (14.4^x speed increase)	10.03 (15.2^x speed increase)	9.62 (14.8^x speed increase)	10.68 (15.0^x speed increase)